

Design of an ultra-compact reference ULE cavity

This content has been downloaded from IOPscience. Please scroll down to see the full text.

2016 J. Phys.: Conf. Ser. 723 012029

(<http://iopscience.iop.org/1742-6596/723/1/012029>)

View [the table of contents for this issue](#), or go to the [journal homepage](#) for more

Download details:

IP Address: 82.225.18.231

This content was downloaded on 11/07/2016 at 14:57

Please note that [terms and conditions apply](#).

Design of an ultra-compact reference ULE cavity

Alexandre Didier¹, Jacques Millo¹, Clément Lacroûte¹, Morvan Ouisse¹, Jérôme Delporte², Vincent Giordano¹, Enrico Rubiola¹ and Yann Kersalé¹

¹ FEMTO-ST, CNRS/UBFC/ENSM/UFM/UTBM, Besançon, France

² CNES, Toulouse, France

E-mail: yann.kersale@femto-st.fr

Abstract. This article presents the design and the conception of an ultra-compact Fabry-Pérot cavity which will be used to develop an ultra-stable laser. The proposed cavity is composed of a 25 mm long ULE spacer with fused silica mirrors. It leads to an expected fractional frequency stability of 1.5×10^{-15} limited by the thermal noise. The chosen geometry leads to an acceleration relative sensitivity below $10^{-12} /(\text{m/s}^2)$ for all directions.

1. Introduction

Ultra-stable lasers are a key element in various applications ranging from optical frequency standards [1, 2], gravitational wave detection [3], tests of fundamental physics [4] and generation of ultra-pure microwave signals [5]. In frequency metrology, and in particular for optical atomic clocks, lasers are stabilized onto ultra-stable Fabry-Pérot cavities providing the relative frequency stability at short integration times in order to probe the atomic transition. The principal limitations of such lasers stems from Fabry-Pérot cavities length fluctuations principally due to thermal and vibration perturbations. Therefore a lot of efforts were dedicated to isolating cavities and making them insensitive to environmental perturbations. Thermal noise floors below 10^{-15} for 100 mm long cavities [6, 7, 8, 9] and of 1×10^{-16} or below for 400 mm long cavity [10] have been already reached. Recently, relative frequency instabilities below 10^{-16} have been obtained by the use of a 480 mm long cavity [11] or with a cryogenic silicon single crystal cavity [12]. In non-laboratory environment, for applications such as the generation of ultra low phase noise microwave for radar [13], geodesy [14] and local oscillator for space missions [15], the relative frequency instability requirements is reduced to the 10^{-15} level surpassing the best quartz crystal oscillator performances. For these fields of applications, a complete redesign of the cavity and its assembly is needed to make the cavity compatible with transport. Recently, several research groups have built cavities that are designed to be vibration-insensitive [16], robust [17] and transportable [15, 18].

In this work, we report the design of a reference cavity with calculated acceleration sensitivities below $10^{-12}/(\text{m/s}^2)$ for all directions. The horizontally oriented cavity is rigidly held with three compressive forces applied in the cavity middle plane (orthogonal to the optical axis). The cavity within a custom made vacuum chamber fits on a $600 \times 300 \text{ mm}^2$ breadboard with a height of 300 mm. The freespace optical components used for the mode matching are directly attached onto this vacuum chamber.



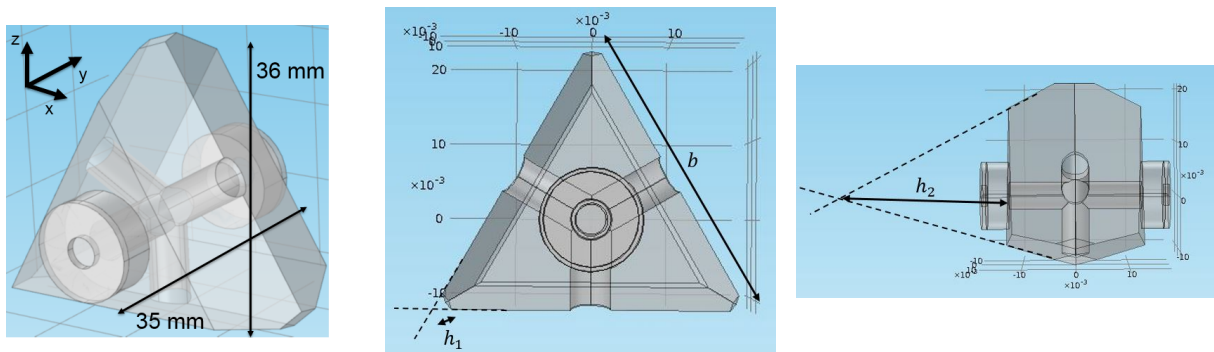


Figure 1. Left: Double tetrahedral spacer with SiO₂ substrates and ULE rings; Center: Cavity front view ; Right: Cavity side view

2. Cavity design and geometry

The optical length of the cavity is 25 mm corresponding to a free spectral range of 6 GHz with a plano-concave optical resonator configuration (radius of curvature of 240 mm). Fused silica mirror substrates are optically contacted to a spacer made of ultra-low expansion (ULE) glass. The overall coefficient of thermal expansion (CTE) is partially compensated by contacting rings in ULE on the back of the mirrors. Thank to the high mechanical quality factor of fused silica, the fractional frequency stability is limited at 1.5×10^{-15} by the thermal noise of the high dielectric reflective coatings for 1.54 μm laser wavelength [19]. It has to be mentioned that the thermal noise can be further reduced using crystalline coatings [20]. This cavity length results from a compromise between the compactness of the cavity and its thermal noise flicker limit. The full size of the final cavity geometry (including mirrors and compensation rings) fits in 35 mm x 36 mm x 41 mm (figure 1). Mechanical simulations using finite element modeling (FEM) have been performed in order to reduce the acceleration sensitivities of the cavity by optimizing its geometry. FEM is also used to dimension the ULE compensation rings to adjust the overall CTE.

2.1. Mechanical modeling

Several geometries have been used for ultra-stable Fabry-Pérot cavities, such as the cylinder [6, 8, 9] and the cube [16] with four holding points. Vertical cavities [7, 9] are held by a monolithically attached midplane ring resting on three Teflon rods or viton. For the spherical cavity, only two holding points on its diameter are used with a "magic angle" [22] where its length is insensitive to the forces used to support it.

We observe the same kind of deformations than those described in [9, 22]. Movements of the mirrors under accelerations can be approximated by a translation along the optical axis (y -axis) and tilts around the two other axis (x -axis or z -axis). For the design of vibration insensitive cavities it is important to keep geometric and stress symmetries. For advantageous geometries the translation do not lead to vibration sensitivity, only remain tilts of the mirrors which can be minimized by tuning the spacer parameters.

In the above-mentioned geometries, such as the cylinder, the measured acceleration sensitivity is always significantly larger for one acceleration direction. In order to further reduce the acceleration sensitivities and to homogenize them, the ends of the cylinder are cut with an angle, thus removing matter near the mirrors. Following this trend, we designed a spacer geometry based on two tetrahedral (see figure 1), allowing to have less matter near the mirrors.

One issue that could increase the acceleration sensitivities of the cavity is the inhomogeneity of the forces used to hold it. To overcome this problem, very careful position adjustments of

the cavity on its supports are needed. With a non hyperstatic three-point holding system, the forces are always self balanced. Our cavity is therefore held in its middle plan on three points. The cavity being held away from the mirrors, the mirrors strains due to the static restraining forces are smaller. The sharp edges of the spacer increase also the stiffness of the spacer and decrease its tendency to bend at its ends.

The double tetrahedral shape of the cavity possesses enough symmetries so that the axial translation of the cavity theoretically vanishes. The biggest strain contribution to the acceleration sensitivities stems therefore from the tilts of the mirrors. The cavity dimensions were optimized through FEM in order to find spacer dimension where the the mirrors tilts could be minimized.

In this article, we focus on the most important parameters on the vibration sensitivity such as the main edge of the spacer b or the depth of cut of the cavity vertices h_1 creating the area for its support (see figure 1). The depth of cut of the end vertices of the cavity h_2 , allowing the attachment of the mirrors on the spacer, have also an impact on the acceleration sensitivity. The diameter of the holes for light propagation and out-gassing decrease slightly the acceleration sensitivities. More importantly, having three holes with 120° axial symmetry instead of just one enables to have the same amplitude of acceleration sensitivity along the three directions.

The parameters were swept in the simulations and the relative length fluctuations of the cavity were extracted from the FEM analysis. We could check that the simulated axial translation of the mirrors is always below $10^{-12}/(\text{m/s}^2)$ (see figure 2), which is at the level of the apparent uncertainty of our simulation. The acceleration sensitivities 1 mm away from the mirrors centers for each transverse direction gave us the contribution of the mirrors rotations to the acceleration sensitivities of the cavity, in the pessimistic case where the optical axis is shifted by 1 mm from the geometric axis of the cavity.

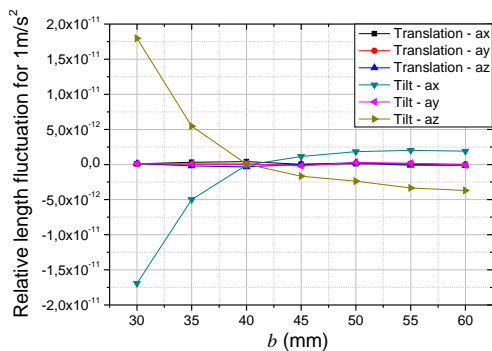


Figure 2. Relative cavity length fluctuation as a function of the main edge of the spacer for the three directions, when the other parameters are fixed ($h_1 = 2$ mm, $h_2 = 35$ mm).

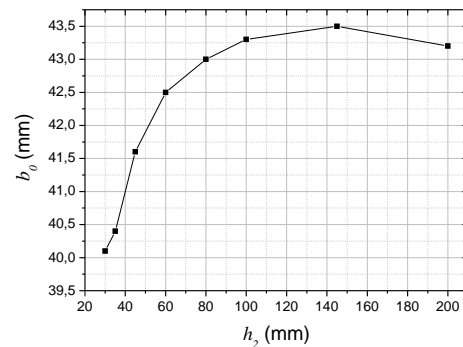


Figure 3. Specific edge length b_0 for several values of h_2 when other parameters are fixed ($h_1 = 2$ mm).

The figure 2 shows an example of vibration sensitivity function as the parameter b . The tilts due to two transverse accelerations (a_x and a_z) vanishes for the same value of the parameter $b_0 = 40$ mm. On figure 3, the values of b_0 is reported as function of the parameter h_2 for a constant value of $h_1 = 2$ mm. This mean that h_2 can be used to tune and minimize b_0 . The cut of depth h_1 also affect the sensitivity due to tilt induced by transverse acceleration (see figure 4) and can be used to optimize the geometry. By tuning b , h_1 and h_2 parameters all together, one can therefore decrease the size of the cavity while maintaining very low acceleration sensitivities.

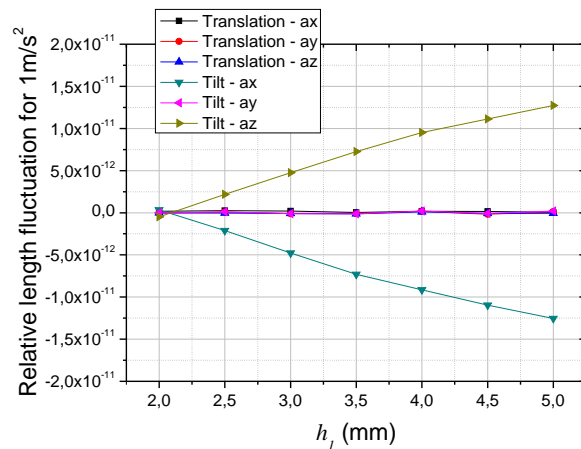


Figure 4. Relative cavity length fluctuation as a function of the depth of cut of the cavity vertices h_1 for the three directions, when the other parameters are fixed ($h_2 = 35$ mm, $b = 41.5$ mm).

The cut angle given by h_2 for a constant length is limited by the surface needed to attach the mirrors to the spacer. The cut depth h_1 has to be superior than 2 mm, in order to be able to hold the cavity on a large enough surface.

All sets of parameters have also an influence on the small offset depicted on figure 2 at the acceleration inversion point. This offset results from the lack of planar symmetry between the x and z -axis.

The best configuration is obtained for a main edge of the spacer $b = 41.5$ mm, a cut depth $h_1 = 2$ mm and a depth of cut of the end vertices of the cavity $h_2 = 35$ mm. With these values we can see that the mirrors relative length fluctuations are below $10^{-12}/(\text{m/s}^2)$ in all directions, even for a strong shift of the optical axis.

2.2. Thermal modeling

The shift of the cavity CTE turning point can be compensated by the use of ULE rings optically contacted to the back of the mirrors [21].

In the present case the mass added on the two ends of the cavity is not negligible compared to the mass of the cavity and influences the vibration sensitivity. Both thermal and mechanical simulations had therefore to be repeated alternatively updating compensation rings and spacer dimensions. Generally speaking, when the mass of the rings increase, the temperature of the overall CTE turning point increase but the vibration sensitivity also tends to rise. A compromise has therefore been made between the thermal and mechanical inversion points.

With further iteration of finite element analysis, ring dimensions of 12.7 mm outer diameter, 5 mm inner diameter and 1 mm thickness has been found to shift the cavity CTE zero crossing near 11°C for the cavity dimensions mentioned in the previous section.

3. Experimental setup

A custom vacuum chamber, with a cubic shape (figure 5) was designed in order to reduce the total volume of the system.

Supporting a transportable cavity by three points only in its middle plan is unsafe. In order to increase the contact surface between the cavity and the holding system, and to add a mechanical

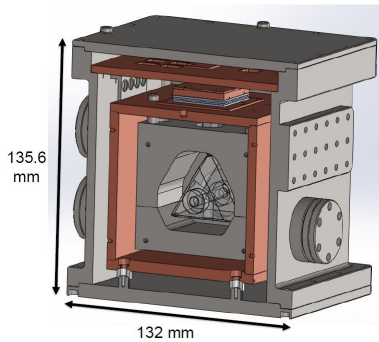


Figure 5. Cavity vacuum chamber.

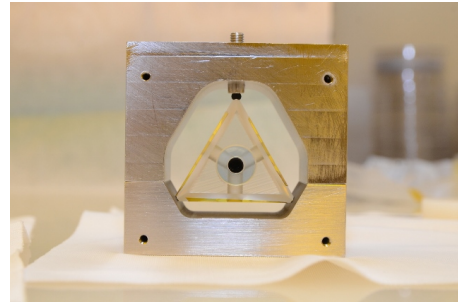


Figure 6. Cavity mounted in its stainless steel support.

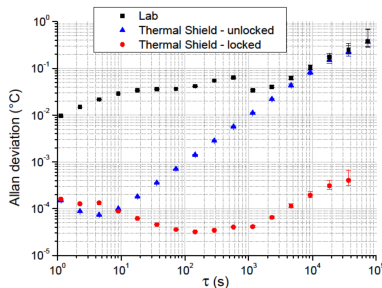


Figure 7. Thermal isolation between the lab and the copper shield.

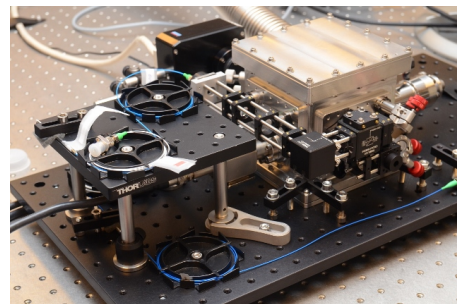


Figure 8. Experimental set-up on a 600 × 300 mm² breadboard.

damping and a good grip, two 2 mm diameter and 1 mm thick Viton pads are placed at the bottom of the enclosure with a re-entrant cutoff of 0.5 mm. A Viton sphere, on the cavity top vertices, of 3.75 mm diameter is used to transfer the force exerted by a home made stud to the cavity (figure 6). The centering of the cavity is managed by eyesight and the positioning errors on each support contact are estimated to be under 0.5 mm. This system has already been able to stand a few g acceleration manually applied in all directions without noticeable sliding movements of the cavity.

To reduce the room temperature influences on the cavity temperature a set of three or four thermal shields are typically used. For a compact and transportable cavity this number of shield has to be considerably reduced. In that way our first thermal shield is the cavity enclosure made in stainless steel in order to get a high thermal capacitance. A second shield in copper will then reduce the thermal radiation from the external environment to the cavity and allow homogeneous temperature around the cavity. To reduce the thermal link between the vacuum chamber and the copper thermal shield, insulating materials (*eg* Teflon and glass reinforced polymer) are used for the posts and the screws holding the thermal shield, in order to provide the needed thermal resistance of 400 K/W per post so that the thermal conduction is reduced to the level of the thermal radiation.

An attenuation of 95 dB is obtained at 1 Hz between the room temperature and the cavity. The thermal time constant was calculated to be around 5 days. Figure 7 shows the experimental result of the copper shield temperature instability. A 40 dB gain is obtained between the room temperature fluctuations and the copper shield. When this shield is temperature controlled the

temperature instability is about 0.1 mK for integration times from 1 s to 10^4 s, compatible with the 10^{-15} level of relative frequency instability for an offset of 1 mK from the CTE inversion.

A 600×300 mm² breadboard is used to support the vacuum chamber containing the cavity. The optics for the cavity mode matching are attached on the vacuum chamber, where custom designed M3 breadboards have been machined. All the fibered optical components used for the laser frequency Pound-Drever-Hall locking are also placed on the breadboard (not seen on figure 8).

4. Conclusion

We reported on the design of an ultra-compact ULE cavity with a thermal noise of 1.5×10^{-15} which fits in a 2.5 liters vacuum chamber. FEM simulations predict acceleration sensitivities below $10^{-12}/(\text{m/s}^2)$ in all directions. The stabilized laser total volume will be of the order of 50 liters. Experimental relative frequency stability and acceleration sensitivities are under investigations.

Acknowledgments

The work has been realized in the frame of the ANR project "Projets d'Investissements d'Avenir (PIA) Equipex Oscillator-Imp" and by CNES. The authors would like to thank the Council of the Région de Franche-Comté for its support to the PIA and to the Labex FIRST-TF for fundings.

References

- [1] Nicholson T L, Campbell S L, Hutson R B, Marti G E, Bloom B J, McNally R L, Zhang W, Barrett M D, Safronova M S, Strouse G F, Tew W L and Ye J 2015 *Nature communications* **6** 6896
- [2] Ushijima I, Takamoto M, Das M, Ohkubo T and Katori H 2015 *Nature Photonics* **9** 185
- [3] Willke B, Danzmann K, Frede M, King P, Kracht D, Kwee P, Puncken O, Savage R L, Schulz B, Seifert F, Veltkamp C, Wagner S, Webels P and Winkelmann L 2008 *Class. Quantum Grav.* **25** 114040
- [4] Herrmann S, Senger A, Mohle K, Nagel M, Kovalchuk E and Peters A 2009 *Phys. Rev. D* **80** 105011.
- [5] Fortier T M, Kirchner M S, Quinlan F, Taylor J, Bergquist J C, Rosenband T, Lemke N, Ludlow A D, Jiang Y, Oates C W and Diddams S A 2011 *Nature Photonics* **5** 425
- [6] Nazarova T, Riehle F and Sterr U 2006 *Appl. Phys. B* **83** 531
- [7] Ludlow A D, Huang X, Notcutt M, Zanon-Willette T, Foreman S M, Boyd M M, Blatt S and Ye J 2007 *Optics Letters* **32** 641
- [8] Webster S A, Oxborrow M, Pugla S, Millo J and Gill P 2008 *Physical Review A* **77** 033847
- [9] Millo J, Magalhães D V, Mandache C, Le Coq Y, English E M L, Westergaard P G, Lodewyck J, Bize S, Lemonde P and Santarelli G 2009 *Physical Review A* **79** 053829
- [10] Swallows M D, Martin J M, Bishof M, Benko C, Lin Y, Blatt S, Rey AM and Ye J 2012 *IEEE Transactions on Ultrasonics, Ferroelectrics, and Frequency Control* **59** 416
- [11] Häfner S, Falke S, Grebing C, Vogt S, Legero T, Merimaa M, Lisdat C and Sterr U 2015 *Optics Letters* **40** 2112
- [12] Kessler T, Hagemann C, Grebing C, Legero T, Sterr U, Riehle F, Martin M J, Chen L and Ye J 2012 *Nature Photonics* **6** 687
- [13] Didier A, Millo J, Grop S, Dubois B, Bigler E, Rubiola E, Lacroûte C and Kersalé Y 2015 *Applied Optics* **54** 3682
- [14] Chou C W, Hume D B, Rosenband T and Wineland D J 2010 *Science* **329** 1630
- [15] Argence B, Prevost E, Lévêque T, Le Goff R, Bize S, Lemonde P and Santarelli G 2012 *Optics Express* **20** 25409
- [16] Webster S and Gill P 2011 *Optics Letters* **36** 3572
- [17] Vogt S, Lisdat C, Legero T, Sterr U, Ernsting I, Nevsky A and Schiller S 2011 *Appl. Phys. B* **104** 741
- [18] Leibrandt D R, Thorpe M J, Bergquist J C and Rosenband T 2011 *Optics Express* **19** 10278
- [19] Numata K, Kemery A and Camp J 2004 *Phys. Rev. Lett.* **93** 250602
- [20] Cole G D, Zhang W, Martin M J, Ye J and Aspelmeyer M 2013 *Nature Photonics* **7** 644
- [21] Legero T, Kessler T and Sterr U 2012 *J. Opt. Soc. Am. B* **27** 914
- [22] Leibrandt D R, Thorpe M J, Notcutt M, Drullinger R E, Rosenband T and Bergquist J C 2011 *Optics Express* **19** 3471